

RESEARCH

Open Access



Green synthesis of silver and iron nanoparticles of isolated proanthocyanidin: its characterization, antioxidant, antimicrobial, and cytotoxic activities against COLO320DM and HT29

Kiran P. Shejawal¹, Dheeraj S. Randive^{1*} , Somnath D. Bhinge², Mangesh A. Bhutkar¹, Ganesh H. Wadkar¹ and Namdeo R. Jadhav³

Abstract

Background: In the current research, we have developed silver and iron nanoparticles of isolated proanthocyanidin (PAC) from grape seed by green synthesis and evaluated for antimicrobial, antioxidant activity and in vitro cytotoxicity against colon cancer cell lines.

Results: One percent solution of isolated proanthocyanidin in water was vigorously mixed with 1% silver nitrate and 1% ferric chloride solution and kept for 4 h, to yield PACAgNP and PACFeNP. The synthesized nanoparticles were characterized by UV, FTIR, XRD, and SEM analysis and evaluated for antimicrobial potential against selected microbes. Moreover, the synthesized nanoparticles were studied for DPPH assay and in vitro cytotoxicity using colon cancer cell lines COLO320DM and HT29 (MTT, SRB, and Trypan blue assay). UV spectroscopy confirmed the development of nanoparticles. SEM analysis showed that the particles were aggregated in the size range of 50 to 100 nm. Antimicrobial potential was found to be less against *Staphylococcus aureus*, *Pseudomonas aeruginosa*, and *Escherichia coli*, whereas cytotoxicity of PACAgNP and PACFeNP against COLO320DM and HT29 exhibited promising results as compared to the pure PAC. PACAgNP and PACFeNP exhibited $20.83 \pm 0.33\%$ and $18.06 \pm 0.60\%$ inhibition, respectively, against DPPH radical, whereas pure PAC showed $16.79 \pm 0.32\%$ inhibition and standard (ascorbic acid) exhibited $98.73 \pm 0.18\%$ inhibition of DPPH radical.

Conclusion: The silver and iron nanoparticles were successfully developed by green synthesis method using isolated proanthocyanidin which is economical and eco-friendly. The use of metal nanoparticles may open up a new opportunity for anticancer therapies to minimize the toxic effects of available anticancer drugs specifically in targeting specific site.

Keywords: Proanthocyanidin, Silver and iron nanoparticles, Antioxidant activity, Cytotoxicity, Colorectal cancer, COLO320DM, HT29

* Correspondence: randivedheeraj@gmail.com

¹Department of Pharmaceutics, Rajarambapu College of Pharmacy, Kasegaon, Walwa, Sangli, Maharashtra 415404, India
Full list of author information is available at the end of the article

Highlights

- The present research work is focused on green synthesis of silver and iron nanoparticles of isolated proanthocyanidin from grape seed extract.
- This is the first attempt to assess scientifically the anticancer efficacy of the developed metal nanoparticles on in vitro colon cell lines HT29 and COLO320DM.
- The results of the study revealed that developed nanoparticles are having significant cytotoxic activity against colon cancer as compared with pure proanthocyanidin (phytoconstituents).
- This is an eco-friendly, economical, easy, and rapid method of development of metal nanoparticles with minimum usage of hazardous chemicals.
- Use of isolated phytoconstituents which are devoid of toxic effects of all other anticancer drugs and better absorption as well as cellular uptake due to nanosize for targeting specific site will be a newer research area.

Background

A foremost reason of cancer death in men and women is colorectal cancer (CRC), and it affects nearly 1 million people throughout the world every year [1]. It is the third most frequently diagnosed cancer in both men and women. About 103,170 new cases and around 51,700 deaths have been estimated to have occurred in 2012 in the USA. The occurrence of CRC in China is lower than that of western countries, but it has increased in the current years and has become a substantial cancer burden in China, mainly in the more developed areas. Epidemiological literature has shown that the daily consumption of fresh fruits and vegetables is connected with a reduced risk of cancer. The special effects may be moderately attributed to the presence of several polyphenolic compounds, which are known to exhibit antioxidant and free radical-scavenging properties [2].

It is very essential to deliver anticancer drug at the site of action, and the dosage form must exhibit high cell penetration or permeability and drug solubility. Nanoparticles may enter the human body via several routes. The probability of penetration depends on the size and surface properties of particles and on the anatomical structure of the specific sites of the exposure routes [3].

Nanotechnology can be termed as the exploitation of matter through specific chemical and/or physical processes to produce materials with specific properties, which can be utilized in particular applications [4, 5]. A nanoparticle can be a microscopic particle or material that has at least one dimension less than 100 nm in size [6–8]. Different bulk materials exhibit sole optical, electrical, thermal, physical, and chemical properties [9], and

hence, they find a range of applications in the areas of environment, medicine, chemistry, energy, agriculture, information, communication, consumer goods, and heavy industry [10, 11]. Recently, there has been a keen interest in the green synthesis of nanoparticles [12].

Owing to the characteristic catalytic and optical properties of the metal nanoparticles as compared to the bulk material, they have fetched greater attention to date in multidisciplinary scientific areas especially in the pharmaceutical, and cosmetic, which position onward growth in commercial interest, and calling for effectual synthesis procedures to match the growing demand of silver, iron, and gold nanoparticles [13].

Ayurvedic and herbal formulations available in the market diverge in quality and therapeutic efficiency owing to the differences in composition of the plant phytoconstituents [14–16]. Advancement in the Ayurvedic herbal medicine has been revolutionized from the showing of phytochemicals and pharmacological activities to elucidating their mechanisms of action and sites of action [17]. Also currently, there is an increased interest in the herbal drugs and remedies for the treatment of chronic diseases [18].

Proanthocyanidins are the naturally available polyphenolic compound(s) which varied in chemical structure, pharmacological action, and characteristics and extensively available in fruits, seeds, vegetables, nuts, flowers, and bark [19].

Grape seed is an abundant source of proanthocyanidin (PACs), which is known to be a powerful inhibitor of aromatase activity; it is an enzyme expressed in higher levels in cancerous than in usual breast tissues [20]. PACs belong to a bigger class of abundant, plant-derived compounds, flavonoids, which offers numerous valuable health effects, largely because of its antioxidant properties [21, 22]. It has been shown to defend against oxidative stress and tobacco-induced DNA damage, and exhibited selective prominent cytotoxicity against some human cancers, including colon, lung, breast, prostate, and gastric carcinomas [23–28].

They are secondary plant metabolites available in many diverse kinds of fruits, vegetables, and plant-based beverages, and also available in cocoa, apple, grapes, tea, and red wine. PAC classes of condensed tannins are oligomers and polymers of (+)-catechin and (–)-epicatechin and other related flavonoids, chiefly linked by either B-type (C4 → C6 or C8) or A-type linkages (C2 → O7). Grape seed extract (GSE) falls into the B-type category, and grape seed extract-rich diets have been connected with a reduced risk of chronic cardiac diseases [29] and also a variety of common cancers, including colorectal cancer [30–32].

Proanthocyanins are strong free radical scavengers and are supposed to be contributors to the health benefits of

fruits and vegetables [33, 34]. Proanthocyanidins obtained from grape seeds have been proven to protect against UV light-induced carcinogenesis, stop immune suppression, enhance interleukin (IL)-12, and decrease IL-10 [35]. Apple PACs have established synergistic effects with lysosomotropic compounds in increasing the anticancer properties targeting human colon cancer-derived metastatic cells [36, 37].

An environmentally friendly option is to prepare nanoparticles dependent on three important parameters, namely solvent medium, reducing and stabilizing or capping agent for NPs [38]. Therefore, the present study is important with respect to the development of metal nanoparticles of phytoconstituent specifically for targeting the cancer. It has many advantages like being eco-friendly and cost-effective, and mainly, the isolated phytoconstituents have prominent activity as compared with extract of plants and their parts; moreover, the side effects of the synthetic drugs can be avoided. Further, in vivo animal study of the metal nanoparticle-based formulation is the new area of research.

Methods

Chemicals

Proanthocyanidin (PAC) was obtained as a gift sample from Influx Healthcare, Mumbai, Maharashtra. All the chemicals used in the study were of analytical grade. Silver nitrate (AgNO_3) and ferric chloride (FeCl_3) were purchased from Loba Chem, Kolhapur. Ciprofloxacin was obtained from Okasa Pharmaceutical, Satara. Cell line COLO320DM and HT29 were procured from NCCS, Pune, Maharashtra.

Microorganism used

The test organisms used in this study were *Staphylococcus aureus* (ATCC 6538), *Pseudomonas aeruginosa*, (ATCC 10145), and *Escherichia coli* (ATCC 8739). The culture was obtained from Yashawantrao Chavan College of Science, Saidapur, Karad (MS), India—415110.

Synthesis of metallic nanoparticles

Synthesis of proanthocyanidin silver nanoparticles (PACAgNPs)

PACAgNPs were synthesized using proanthocyanidin solution and AgNO_3 solution in accordance with the procedure mentioned by Phull et al. with minor modification [39]. Equal volumes (1:1) of 1% proanthocyanidin aqueous solution and 1% silver nitrate solution were incubated at ambient temperature for 2–3 h to obtain PACAgNPs. Synthesis of PACAgNPs was detected by naked eye with a change of color from dark red to faint brown, which was confirmed by UV spectroscopy. The collected PACAgNPs were centrifuged for 10 min at 10,

000 rpm and dried in vacuum chamber at 35 °C shown in Fig. 1.

Synthesis of proanthocyanidin iron nanoparticles (PACFeNPs)

For the synthesis of ProFeNPs, proanthocyanidin aqueous solution and ferric chloride solution were used in accordance with the procedure mentioned by Raju et al. [40] with minor modification. Ferric chloride (1%) and proanthocyanidin solution (1%) were vigorously combined in a ratio of 1:1. The mixture was then placed on an orbital shaker for 24 h at an ambient temperature to obtain PACFeNPs. The synthesis of PACFeNPs was observed with a color change from dark black to dark brown, which was also confirmed by UV spectroscopy. The collected PACFeNPs were centrifuged for 10 min at 10,000 rpm and dried in vacuum chamber at 35 °C shown in Fig. 1.

Characterization of nanoparticles

UV-Vis absorbance of PAC, PACAgNP, and PACFeNP

The development of metal nanoparticles of PACAgNP and PACFeNP by the proanthocyanidin was recorded periodically using a UV spectrophotometer (Shimadzu). The samples were diluted with 2 mL of deionized water and measured for UV-Vis spectrum after the formation of nanoparticles that change in color. Deionized water was used as a blank for background correction. All samples were scanned from 200 to 800 nm.

SEM and histogram analysis of PACAgNP and PACFeNP

Scanning electron microscopy (SEM) is a normally used method of evaluation and morphological analysis of nanoparticles at the nanometer to micrometer scale. Developed PACAgNP and PACFeNP were characterized using a high-resolution scanning electron microscope (Schottky field emission scanning microscope SU5000). The samples were prepared by a simple drop coating of suspended gold solution on to an electric clean glass and allowed the solvent to evaporate, and the samples were dried at room temperature and analyzed in a microscope.

FTIR spectroscopy analysis of PAC, PACAgNP, and PACFeNP

To recognize the different biomolecules present in the proanthocyanidin and the phytocompounds in Ag and Fe, nanoparticles after synthesis were analyzed by FTIR (Bruker Alpha Echo ATR). Spectrum was recorded in the range of 400–4000 cm^{-1} .

XRD analysis of PACAgNP and PACFeNP

The green synthesized silver and iron nanoparticles of PAC were evaluated by XRD analysis using an XRD-6000 X-ray diffractometer (Bruker D8 discover) operated

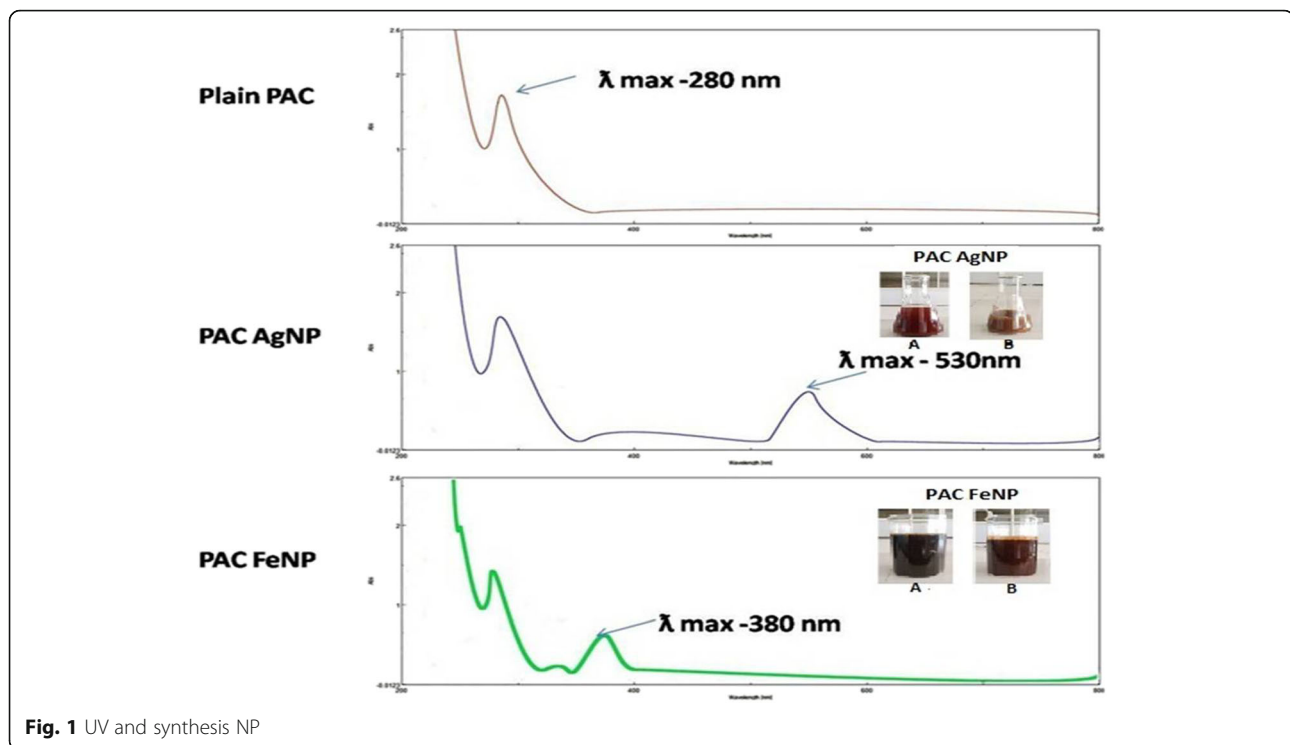


Fig. 1 UV and synthesis NP

at a voltage of 40 kV and 30 mA with Cu K α radiation in θ – 2θ configurations. The crystalline size was determined from the width of the XRD peaks by assuming that they were free from non-uniform strains.

Antimicrobial activity of PAC, PACAgNP, and PACFeNP

In vitro antimicrobial activity was performed using the agar well diffusion technique [41]. The sterile agar was inoculated with the bacterial culture (*S. aureus*, *P. aeruginosa*, and *E. coli*) for 48 h at 37 °C. Antimicrobial activities were tested on nutrient medium against *S. aureus*, *P. aeruginosa*, and *E. coli*, which are representative types of Gram-positive and Gram-negative organisms. Wells were bored by using a sterile borer. Standard solution (ciprofloxacin) and test samples PAC, PACAgNP, and PACFeNP (5 mg/mL was prepared by dissolving the test sample in DMSO) were placed into the wells (80 μ L). Plates were then kept for 2 h in the refrigerator to enable prediffusion of the extracts into the agar. Finally, the plates were incubated overnight (24 h at 37 °C.) The antimicrobial activity was determined by measuring the diameter of zone of inhibition [42, 43].

In vitro cytotoxicity studies of PAC, PACAgNP, and PACFeNP by using MTT assay

Human HT29 cell and COLO320DM were obtained from the National Center for Cell Sciences, Pune, MS, India, 411007. The cell cultures were maintained in DMEM supplemented with 10% fetal bovine serum. The

cells were plated at a density of 1×10^4 cells per well in a 96-well plate and cultured for 24 h at 37 °C. The cells were subsequently exposed, the plates were incubated for 24 h, and cell proliferation was measured by adding 10 μ L of MTT (thiazolyl blue tetrazolium bromide) dye (5 mg/mL in phosphate-buffered saline) per well. The plates were incubated for a further 4 h at 37 °C in a humidified chamber containing 5% CO₂. Formazan crystals formed due to reduction of dye by viable cells in each well were dissolved in 200 μ L DMSO, and absorbance was read at 490 nm.

Finally, the percent cytotoxicity of the compounds was calculated by using the following formula:

$$\text{Percent Cytotoxicity} = \frac{\text{Reading of control} - \text{Reading of treated cells}}{\text{Reading of control}} \times 100$$

Since the absorbance was directly associated with the number of viable cells, the percent viability was determined from the absorbance.

In vitro cytotoxicity studies of PAC, PACAgNP, and PACFeNP by using SRB assay

Human HT29 cells and COLO320DM were maintained in DMEM supplemented with 10% fetal bovine serum. The cells were plated at a density of 1×10^4 cells per well in a 96-well plate and cultured for 24 h at 37 °C. The cells were subsequently exposed to 100 μ g/mL compound. After drug incubation, 50 μ L TCA (50%) was kept for 1 h at 4 °C. Then, the plate was washed with

TDW (triple distilled water) and air dried. Thereafter, 100 μL SRB dye was added in each well and kept for 30 min at room temperature. Again, the plate was washed three times with 1% acetic acid and air dried. Finally, 200 μL Tris buffer was added, and the absorbance was read at 490 nm.

The percent cytotoxicity of the compounds was calculated by using following formula:

$$\text{Percent Cytotoxicity} = \frac{\text{Reading of control} - \text{Reading of treated cells}}{\text{Reading of control}} \times 100$$

In vitro cytotoxicity studies of PAC, PACAgNP, and PACFeNP by using Trypan blue assay

The dye exclusion test is used to find out the number of viable cells present in a cell suspension. It is based on the principle that live cells possess undamaged cell membranes that exclude certain dyes, such as Trypan blue, eosin, or propidium, whereas dead cells do not exclude. In this test, a cell suspension is simply mixed with Trypan blue dye and then visually examined to determine whether cells take up or exclude dye. In the study presented here, a viable cell will have undamaged a clear cytoplasm whereas a non-viable cell will have a blue cytoplasm.

Fifty microliters of cell lines of human HT29 cells and Colo 320 D was taken in micro-centrifuge tube. They were incubated for 3 min and then added 50 μL of all samples of nanoparticles in concentration of 100 $\mu\text{g mL}^{-1}$ which were prepared by dissolving in phosphate buffer pH 7.4 and DMSO. They were incubated in CO_2 incubator for 3 min, and thereafter, Trypan blue (0.4%) 50 μL was added in each tube. They were further incubated for 3 min in CO_2 incubator and analyzed for total viable cells and non-viable cells by using Nubars slide [44].

Antioxidant activity of PAC, PACAgNP, and PACFeNP, by DPPH (2,2-diphenyl-2-picryl hydrazyl hydrate) assay

The scavenging ability of PAC, PACAgNP, and PACFeNP on the stable free radical was calculated with the method expressed by Mensor et al. [45]. Twenty microliters of PAC, PACAgNP, and PACFeNP solutions was separately added in three labeled test tubes. Subsequently, 0.5 mL of methanolic solution of DPPH and 0.48 mL of methanol were added to each test tube, after which all tubes were allowed to react at an ambient temperature for 30 min. The control was prepared as described above, without any extract and nanoparticles. Methanol was used to correct the baseline. After 30 min of incubation, the discoloration of the purple color was measured under a UV-Visible spectrophotometer. The radical-scavenging activity was determined by the following formula [45]:

$$\text{Scavenging activity (\%)} = \frac{A_{\text{abs}}(\text{Control}) - A_{\text{abs}}(\text{Sample})}{A_{\text{abs}}(\text{Control})} \times 100$$

where A (control) is the absorbance of control sample PACAgNP and PACFeNP measured at 530 nm and 275 nm, respectively, and A (control) is the absorbance of PAC measured at 280 nm.

Statistical analysis

Statistical data of the cytotoxicity were assessed on GraphPad Prism 8 for Windows 64 bit with version 8.0.1 (244). Results were analyzed by one-way ANOVA with Dunnett's post-test analysis of variance. The mean standard error mean (SEM) of all calculated values was shown in each group. A value of $P < 0.05$, 0.01, or 0.001 was considered statistically significant.

Results

UV-Vis spectroscopy of PAC, PACAgNP, and PACFeNP

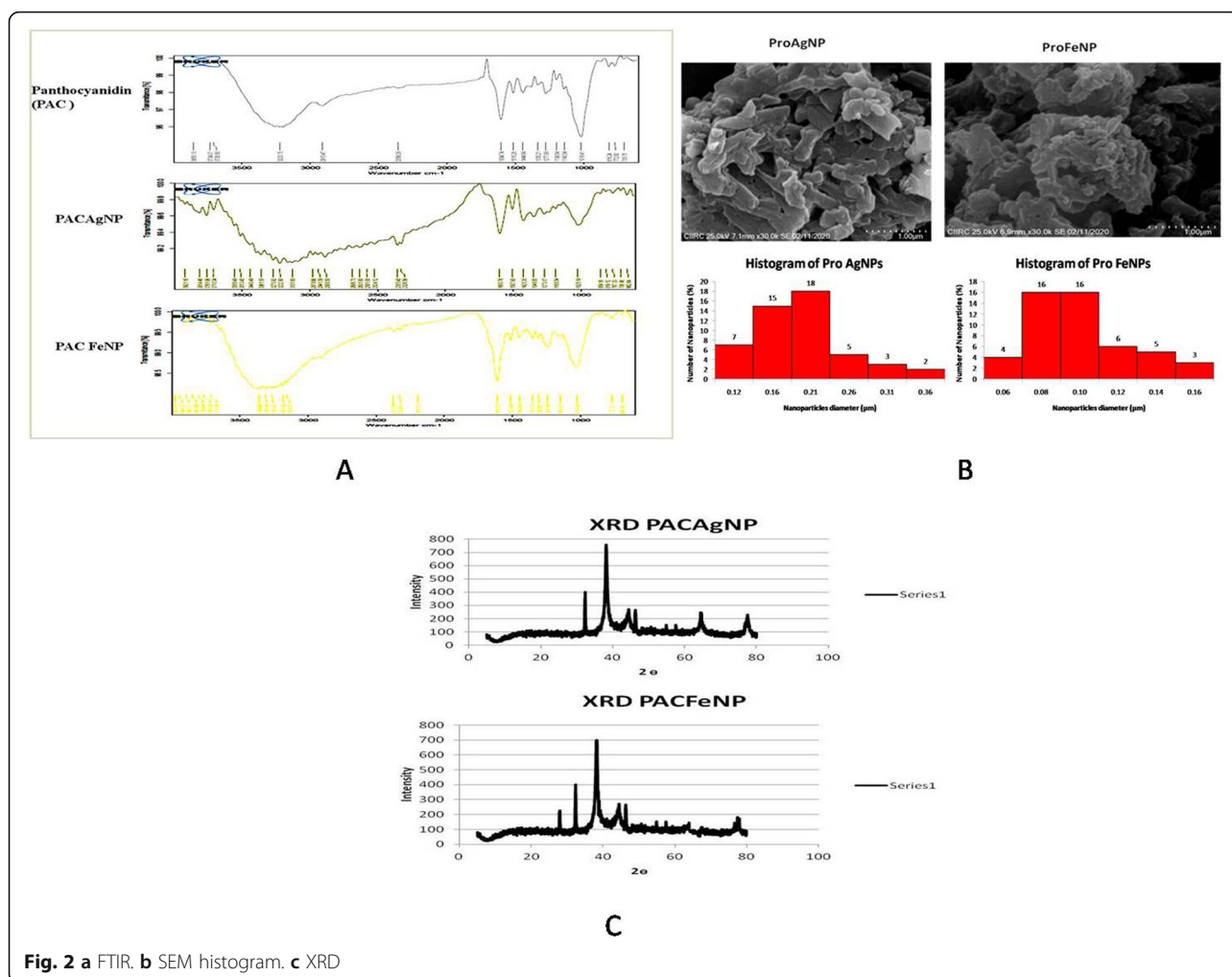
When the aqueous PAC was mixed with aqueous AgNO_3 and FeCl_3 solution, the color of the solution changed which indicated the formation of silver and iron nanoparticles. This change in color was due to the collective coherent oscillation of conduction electrons at the surface of the nanoparticles that interact with the oscillating electric field of the incident light, a phenomenon called surface plasmon resonance (SPR). This change in color indicated the reduction of Ag and Fe ions which was traced with UV-Vis spectroscopy. The PAC showed max at 280 nm, and silver nanoparticle PACAgNP possesses specific wavelength that can absorb at max 530 nm, whereas iron nanoparticles PACFeNP exhibit max at 380 nm as shown in Fig. 1.

FTIR spectrum of PAC, PACAgNP, and PACFeNP

In the FTIR of proanthocynidin, fairly sharp peaks at 3223.75, 2910.47, 1604.74, 1515.78, 1444.64, 1217.89, and 1018.41 cm^{-1} were observed, which indicate the presence of the functional group present in the compound. However, the aromatic at 1604.74 (C-C-valence) cm^{-1} , the OH phenolic at 3223.75 (O-H-valence) and 2910.47 (C-H-valence, arene), alkane (OCH_3), the methoxylic at 1217.89 cm^{-1} , and C-O stretching at 1044.64 appeared in the IR spectrum of complex as shown in Fig. 2a.

PACAgNP

These characteristic vibrations after reduction of Ag+ ions were shifted to new peaks at 3222.80, 2888.50, 1600.76, 1507.93, 1425.35, 1188.54, and 1025.79 cm^{-1} , which indicated the presence of the functional group present in the compound. However, the aromatic at 1600.76 (C-C-valence) cm^{-1} , the OH phenolic at 3222.80 (O-H-valence) and 2888.50 (C-H-valence,



arene), alkane (OCH₃), the methoxylic at 1188.54 cm⁻¹, and C-O stretching at 1025.79 appeared in the IR spectrum of complex as shown in Fig. 2a.

In addition, bio-reduction showed that the 3222.80, 2888.50, and 1025.79 cm⁻¹ bands were suppressed in the AgNP. Proanthocyanidin and NPs showed similar absorption bands, indicating that NPs might be stabilized by proanthocyanidin. On the basis of the orange, yellow, and brownish green color of the biomass and the groups suggested by FTIR analysis, it was hypothesized that proanthocyanidin may be involved in silver nanoparticle synthesis.

PACFeNP

These characteristic vibrations after reduction of Fe³⁺ ions were shifted to new peaks at 3310.40, 2900.05, 1610.53, 1513.64, 1448.60, 1149.07, and 1025.38 cm⁻¹, which indicated the presence of the functional group present in the compound. However, the aromatic at 1610.53 (C-C-valence) cm⁻¹, the OH phenolic at 3310.40 (O-H-valence) and 2900.05 (C-H-valence,

arene), alkane (OCH₃), the methoxylic at 1149.07 cm⁻¹, and C-O stretching at 1025.38 appear in the IR spectrum of complex as shown in Fig. 2a. In addition, bio-reduction showed that the 3310.40, 2900.05, and 1149.07 cm⁻¹ bands were suppressed in the FeNP. Proanthocyanidin and NPs showed similar absorption bands, indicating that NPs might be stabilized by proanthocyanidin. On the basis of the orange, yellow, and blackish color of the biomass and the groups suggested by FTIR analysis, it was hypothesized that proanthocyanidin may be involved in iron nanoparticle synthesis.

SEM and histogram analysis of PACAgNP and PACFeNP

A scanning electron microscope was used to analyze the structure of PACAgNP and PACFeNP nanoparticles that are developed and represented in Fig. 2b. The nanoparticles formed were aggregated having a size range of 100 to 120 nm. This aggregation of the nanoparticles can be minimized or prohibited by increasing the concentration of the proanthocyanidin extract. Histograms of both the nanoparticles have been represented in Fig. 2b exhibiting

average particle size PACFeNP $0.09083 \pm 0.02627 \mu\text{m}$ and PACAgNP $0.17746 \pm 0.05784 \mu\text{m}$.

XRD spectrum of PACAgNP and PACFeNP

The XRD pattern of the synthesized silver and iron nanoparticles formed using proanthocyanidin is shown in Fig. 2c. The diffraction peak at $2\theta = 38^\circ$ and subsequent higher order reflections can be indexed to the Ag and other facets of silver nanoparticles by comparing JCPDS file no: 89-3722; in case of PACFeNP, the peak shown at $2\theta = 33^\circ$ corresponds to the iron compared with standard XRD for iron (JCPDS data: pdf no 39:1346).

The XRD spectrum also revealed a weak peak around $2\theta = 30^\circ$, which can be attributed to the phytochemical components. It, thus, confirmed that the nanoparticles formed on the membrane consisted of crystalline. XRD indicated possible multicomponent product formation at higher energy.

Antibacterial activity of PAC, PACAgNP, and PACFeNP

The zones of inhibition revealed that there is very little antimicrobial potential of PAC, PACAgNP, and PACFeNP against *Pseudomonas aeruginosa*, *Staphylococcus aureus*, and *E. coli*. The results are highlighted in Table 1, and the zone of inhibition is depicted in Fig. 3.

Results of cytotoxicity of PAC, PACAgNP, and PACFeNP

The results of cytotoxicity assay by MTT and SRB assay have been presented in Table 2 with respect to two different colon cancer cell lines namely COLO320DM and HT29. A variation in the results of different assay was observed; however, the silver nanoparticles exhibited better activity than pure PAC in both the methods. The results of MTT assay against HT29 demonstrated that PACAgNP showed maximum $63.34 \pm 1.64\%$ inhibition represented in Fig. 4x (A). In case of COLO320DM, silver nanoparticles exhibited $64.27 \pm 1.63\%$ inhibition as represented in Fig. 4x (B), whereas the SRB assay of PAC, PACAgNP, and PACFeNP against HT29 revealed $69.21 \pm 1.86\%$ inhibition by PACAgNP as shown in Fig. 4x (C). In case of COLO320DM SRB assay, a maximum of $71.6 \pm 1.97\%$ inhibition was exhibited by silver nanoparticles as depicted in Fig. 4x (D).

The results of Trypan blue assay revealed that silver nanoparticles PACAgNP showed $85.63 \pm 0.27\%$ non-viability of COLO320DM cell line when observed on a Motic microscope, whereas iron nanoparticles PACFeNP exhibited $94.57 \pm 0.36\%$ inhibition of HT29 cell lines as represented in Table 3.

Results of DPPH (2,2-diphenyl-2-picryl hydrazyl hydrate) assay of PAC, PACAuNP, and PACFeNP

The DPPH activity results demonstrated effective free radical percent scavenging potential of PAC, PACAuNP, and PACFeNP as depicted in Fig. 4y. As compared to ascorbic acid (standard), the concentration response curves of DPPH radical-scavenging activity of PAC, PACAuNP, and PACFeNP are shown in Table 4. It was observed that PACAgNPs were more effective than PAC extract and PACFeNPs. At a concentration of $50 \mu\text{g mL}^{-1}$, the scavenging activity of PACAgNPs was observed to be $20.83 \pm 0.33\%$, while at similar concentration, for the PACFeNPs it was reported to be $18.06 \pm 0.60\%$. The outcome of antioxidants on DPPH is thought to be due to their hydrogen donating ability.

Discussion

Engineered nanomaterials showed imperative benefits due to their unique nanostructure, along with their significant properties for the designed applications [46]. Metallic NPs have been synthesized using several different methods such as chemical reduction, electrochemical, microbiological reduction, ultrasonication method, and microwave radiation [47]. The present research work is focused on green synthesis of silver and iron nanoparticles of isolated proanthocyanidin from grape seed extract. It is an eco-friendly, economical, easy, and rapid method of development of metal nanoparticles with minimum usage of hazardous chemicals. The developed silver and iron nanoparticles were characterized by UV spectroscopy which showed the change in absorbance after development of nanoparticles. FTIR spectrum provides the information about the chemical change of the functional groups involved in bio-reduction [48, 49]. The FTIR spectra of developed nanoparticles confirmed the formation of silver and iron nanoparticles as characteristic vibrations after reduction of Ag^+ ions were

Table 1 Results of antibacterial activity of PAC, PACAgNP, and PACFeNP against selected microbial strains

Sr. no.	Sample name	Zone of inhibition diameter (mm) against the selected microorganisms		
		<i>Pseudomonas aeruginosa</i>	<i>Staphylococcus aureus</i>	<i>E. coli</i>
1	PAC pure	6.00 ± 0.10	0.0	0.00
2	PACAgNP	7.0 ± 0.11	12.00 ± 0.16	6.00 ± 0.13
3	PACFeNP	6.0 ± 0.14	6.0 ± 0.12	0.00
4	Ciprofloxacin std.	35 ± 0.11	38 ± 0.13	40 ± 0.12

Values are expressed in triplicate mean SD

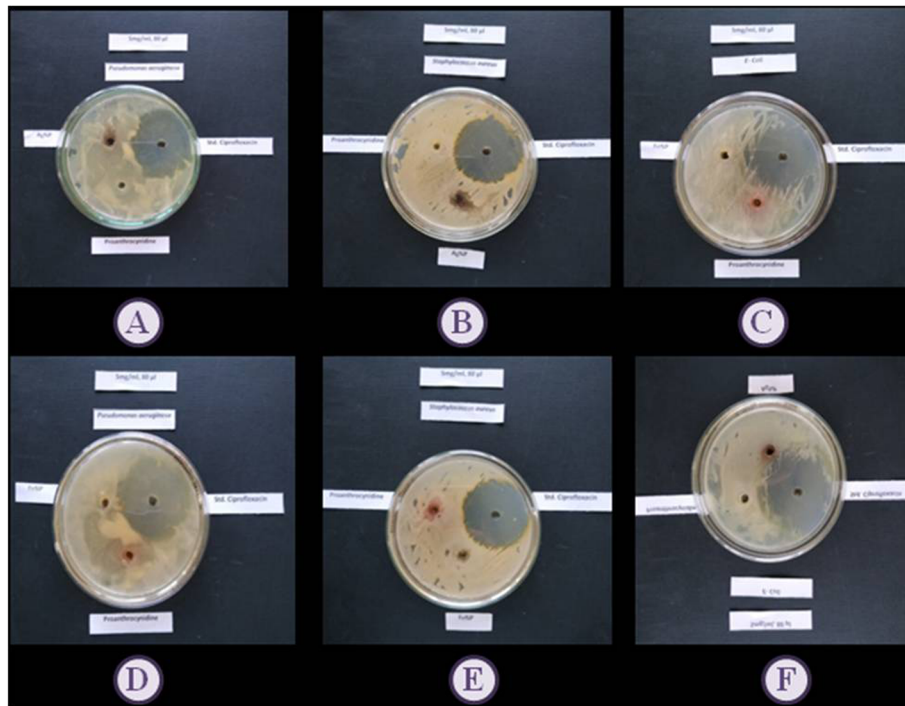


Fig. 3 Antimicrobial activity

shifted to new peaks at 3222.80, 2888.50, 1600.76, 1507.93, 1425.35, 1188.54, and 1025.79 cm^{-1} . And characteristic vibrations after reduction of Fe^{3+} ions were shifted to new peaks at 3310.40, 2900.05, 1610.53, 1513.64, 1448.60, 1149.07, and 1025.38 cm^{-1} . Also,

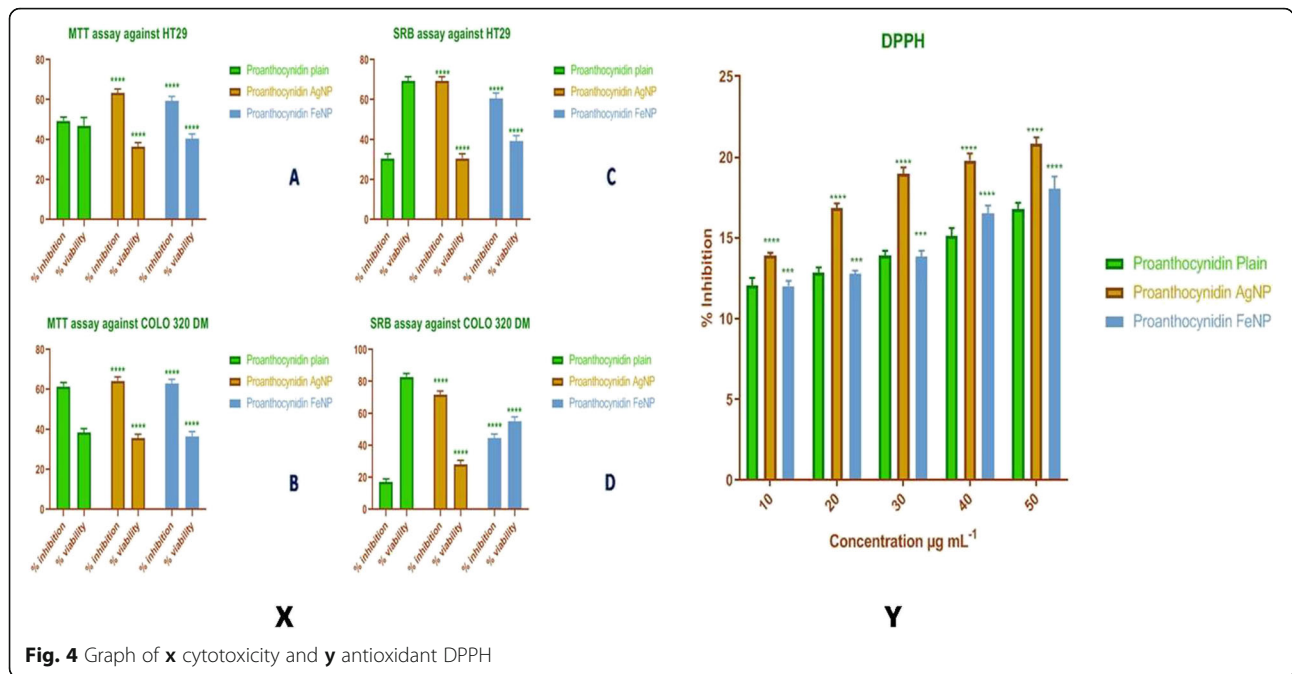
characteristic color change can be attributed to the surface plasmon resonance of deposited AgNPs. And it clearly indicated the development of nanoparticles [50].

The size of nanoparticles and its morphology were clearly observed in the SEM images. The average size for

Table 2 Results of cytotoxicity of PAC, PACAgNPs, and PACFeNP by MTT and SRB assay using COLO320DM and HT29 cell lines

Compound	Mean OD	Percent inhibition	Percent viability
MTT assay against HT29 (control—0.321)			
Proanthocynidin plain	0.161	49.53 ± 1.54	47.13 ± 3.32
Proanthocynidin AgNP	0.117	63.34 ± 1.64	36.65 ± 1.64
Proanthocynidin FeNP	0.129	59.39 ± 1.84	40.60 ± 1.84
MTT assay against COLO320DM (control—0.384)			
Proanthocynidin plain	0.146	61.49 ± 1.66	35.51 ± 1.66
Proanthocynidin AgNP	0.137	64.27 ± 1.63	35.72 ± 1.63
Proanthocynidin FeNP	0.142	63.17 ± 1.63	36.49 ± 2.07
SRB assay against HT29 (control—0.292)			
Proanthocynidin plain	0.204	30.71 ± 1.88	69.29 ± 1.88
Proanthocynidin AgNP	0.090	69.21 ± 1.86	30.78 ± 1.86
Proanthocynidin FeNP	0.115	60.57 ± 2.20	39.43 ± 2.20
Proanthocynidin plain	0.204	30.71 ± 1.88	69.29 ± 1.88
SRB assay against COLO320DM (control—0.252)			
Proanthocynidin plain	0.209	17.11 ± 1.72	82.89 ± 1.72
Proanthocynidin AgNP	0.073	71.6 ± 1.97	28.4 ± 1.97
Proanthocynidin FeNP	0.141	44.60 ± 2.18	55.39 ± 2.18

Values are expressed in triplicate mean SD



PACFeNP was observed to be $0.09083 + 0.02627 \mu\text{m}$ and $0.17746 + 0.05784 \mu\text{m}$ for PACAgNP. The XRD results revealed weak peak at $2\theta = 30^\circ$ for phytoconstituent, whereas diffraction peak at $2\theta = 38^\circ$ was observed for silver nanoparticles and iron nanoparticles showed the peak at $2\theta = 33^\circ$.

In case of antimicrobial activity, the developed silver and iron nanoparticles exhibited little antimicrobial potential as compared to pure proanthocyanidin. Metal NPs increase the antibacterial potential due to the formation of reactive oxygen species (ROS), developed from different types of iron oxide nanoparticles like FeO, Fe₂O₃, and Fe₃O₄. The free radical produced in the reaction causes intracellular stresses that can damage the DNA of the cell [51].

The in vitro cytotoxicity results against HT29 and COLO320DM showed that PACAgNP exhibited $63.34 \pm 1.64\%$ inhibition (MTT assay) and $69.21 \pm 1.86\%$ inhibition (SRB assay) against HT29. In case of COLO320DM, PACAgNP demonstrated $64.27 \pm 1.63\%$ inhibition (MTT assay) and $71.6 \pm 1.97\%$ inhibition (SRB assay).

In DPPH assay, PACFeNP and PACAgNP exhibited $18.06 \pm 0.60\%$ and $20.83 \pm 0.33\%$ inhibition, respectively.

The obtained parameters of the characterization and evaluation of the nanoparticles clearly revealed that as compared to proanthocyanidin, the silver and iron nanoparticles possess better antioxidant and anticancer potential against colorectal cancer. Thus, the use of isolated phytoconstituent(s) which are devoid of side effects and promoting better absorption and cellular uptake owing to their nanosize will certainly achieve effective targeting and has to be provided greater attention as a newer research area. Also, several review papers have been published about the synthesis of silver nanoparticles using natural polymers like k-Carrageenan and synthetic polymers like poly vinyl pyrrolidone and polyethylene glycol to improve the strength and stability of nanoparticles. As per the study of Moustafa, the use of natural and synthetic polymer for the development of silver nanoparticles opened up new research area in medicinal and biological field along with food industry [52].

Conclusion

We have successfully synthesized PACAgNPs and PAC-FeNPs using proanthocyanidin isolated from grape seed extract by employing a green synthesis method which is

Table 3 Results of cytotoxicity of PAC, PACAgNPs, and PACFeNP by using Trypan blue assay

Sr. no	Drug	COLO320DM		HT29	
		Percent viability	Percent non-viable	Percent viability	Percent non-viable
1	Proanthocyanidin plain	31.45 ± 0.49	68.88 ± 0.36	25.48 ± 0.31	74.70 ± 0.58
2	Proanthocyanidin AgNP	14.89 ± 0.30	85.63 ± 0.27	9.56 ± 0.26	90.23 ± 0.43
3	Proanthocyanidin FeNP	25.7 ± 0.42	74.5 ± 0.28	5.34 ± 0.18	94.57 ± 0.36

Values are expressed in triplicate mean SD

Table 4 Antioxidant activity of DPPH radical-scavenging activity

Concentrations, $\mu\text{g mL}^{-1}$	Standard, percent inhibition	PAC, percent inhibition	PACAgNPs, percent inhibition	PACFeNPs, percent inhibition
10	93.29 \pm 0.60	12.07 \pm 0.37	13.92 \pm 0.13	12.01 \pm 0.27
20	95.13 \pm 0.54	12.86 \pm 0.25	16.83 \pm 0.24	12.78 \pm 0.16
30	96.16 \pm 0.17	13.89 \pm 0.24	18.95 \pm 0.33	13.83 \pm 0.30
40	97.76 \pm 0.29	15.11 \pm 0.41	19.80 \pm 0.35	16.52 \pm 0.40
50	98.73 \pm 0.18	16.79 \pm 0.32	20.83 \pm 0.33	18.06 \pm 0.60
IC50	–	12.50 \pm 0.30	7.37 \pm 0.27	9.31 \pm 0.22

Values are expressed in triplicate mean SD

relatively simple and environmentally benign. PACAgNPs and PACFeNPs were obtained, with particles between 50 and 100 nm in size. It is easy and cost-effective and does not involve any harmful and poisonous chemicals. All the other characterization like UV, FTIR, XRD, and SEM confirmed the development of nanoparticles. We have observed significant antioxidant activity and free radical-scavenging capacities. PACAgNPs and PACFeNPs exhibited a little antibacterial activity against the selected strains of microbes. In a nutshell, the study showed that the developed NPs from the isolated PAC exhibit beneficial antioxidant and anticancer potential when assessed by three different in vitro assay methods with specifically colon cancer cell lines. Thus, it may open up a new opportunity for anticancer therapies that need further research.

Abbreviations

PAC: Proanthocyanidin; PACAgNP: Proanthocyanidin silver nanoparticle; PACFeNP: Proanthocyanidin iron nanoparticle; UV: Ultraviolet visible spectroscopy; FTIR: Fourier transform infrared spectroscopy; XRD: X-ray diffraction; SEM: Scanning electron microscope; DMEM: Dulbecco's modified Eagle's medium; DPPH: 2,2-Diphenyl-2-picryl hydrazyl hydrate; MTT: 3-(4,5-Dimethylthiazol-2-yl)-2,5-diphenyltetrazolium bromide; SRB: Sulforhodamine B

Acknowledgements

The authors are thankful to the Secretary of KES Society Kasegaon, and Principal of Rajarambapu College of Pharmacy, Kasegaon, Sangli, Maharashtra, for providing facilities. We are also thankful to the managing director *Influx Healthcare, Mumbai*, for providing pure phytoconstituent markers. Dr. Sandip Patil MD Biocyte Institute of Research and Development (BiRD) Sangli MH

Authors' contributions

The work was carried out by DSR during the period of study for the degree of doctor of philosophy under the supervision of SDB. All the laboratory work including preparation and results has been carried out by KPS and DSR. The analysis and interpretation of the results were carried out by MAB, GHW, and NRJ. The manuscript was written by KPS and revised by DSR and SDB. All the authors have read and approved the manuscript.

Funding

No any funding received for this work.

Availability of data and materials

All the data required for the processing of the conclusions are presented in the "Results" section. Supporting data was included separately.

Ethics approval and consent to participate

Not applicable

Consent for publication

Not applicable

Competing interests

The authors declare that they have no competing interests.

Author details

¹Department of Pharmaceutics, Rajarambapu College of Pharmacy, Kasegaon, Walwa, Sangli, Maharashtra 415404, India. ²Department of Pharmaceutical Chemistry, Rajarambapu College of Pharmacy, Kasegaon, Walwa, Sangli, Maharashtra 415404, India. ³Department of Pharmaceutics, Bharati Vidyapeeth College of Pharmacy, Kolhapur, Maharashtra 416013, India.

Received: 27 May 2020 Accepted: 4 August 2020

Published online: 20 August 2020

References

- Jemal A, Murray T, Ward E (2005) Cancer statistics. *CA Cancer J Clin* 55:10–30
- Huang S, Yang N, Liu Y, Gao J, Huang T, Hu L, Zhao J, Li Y, Li C, Zhang X (2012) Grape seed proanthocyanidins inhibit colon cancer-induced angiogenesis through suppressing the expression of VEGF and Ang1. *Int J Mol Med* 30:1410–1416
- Todkar SS, Bhutkar MA, Randive DS, Wadkar GH, Bhinge SD (2017) Risk and management of nanoparticles - an overview. *Int J Phar Res Life Sci* 1:1–13
- Environmental Protection Agency, (2007). "Nanotechnology white paper," USEPA 100/B-07/001.
- Chavan RR, Bhinge SD, Bhutkar MA, Randive DS, Wadkar GH, Todkar SS, Urade MN (2020) Characterization, antioxidant, antimicrobial and cytotoxic activities of green synthesized silver and iron nanoparticles using alcoholic *Blumea eriantha* DC plant extract. *Mater Today Commun* 24:101320. <https://doi.org/10.1016/j.mtcomm.2020.101320>
- Sulaiman GM, Hussien HT, Saleem MM (2015) Biosynthesis of silver nanoparticles synthesized by *Aspergillus flavus* and their antioxidant, antimicrobial and cytotoxicity properties. *Bull Mater Sci* 38(3):639–644
- Al-Shmgani HSA, Mohammed WH, Sulaiman GM, Saadoon AH (2017) Biosynthesis of silver nanoparticles from *Catharanthus roseus* leaf extract and assessing their antioxidant, antimicrobial, and wound-healing activities. *Artif Cell Nanomed B* 45(6):1234–1240. <https://doi.org/10.1080/21691401.2016.1220950>
- Thakkar KN, Mhatre SS, Parikh RY (2010) Biological synthesis of metallic nanoparticles. *Nanomedicine* 6:257–262
- Panigrahi S, Kundu S, Ghosh SK, Nath S, Pal T (2004) General method of synthesis for metal nanoparticles. *J Nanopart Res* 6:411–414
- The Energy and Resources Institute (2010) Nanotechnology development in India: building capability and governing the technology. Briefing Paper, TERI
- Herlekar M, Barve S, Kumar R (2014) Plant-mediated green synthesis of iron nanoparticles. *J Nanomater*:1–9
- Biao L, Tan S, Zhang X, Gao J, Liu Z, Fu Y (2018) Synthesis and characterization of proanthocyanidins-functionalized Ag nanoparticles. *Colloids Surf B: Biointerfaces* 169:438–443
- Gurushankar K, Gohulkumar M, Prasad NR, Rishnakumar N (2014) Synthesis, characterization and in vitro anti-cancer evaluation of hesperetin-loaded nanoparticles in human oral carcinoma (KB) cells. *Adv Nat Sci Nanosci Nanotechnol* 5:1–10

14. Randive DS, Sayyad SF, Bhinge SD, Bhutkar MA (2016) Preparation of Arjunāriṣṭa using microbes isolated from woodfordia fruticosa flowers (dhayati). *Anc Sci Life* 36:42–47
15. Randive DS, Bhinge SD, Bhutkar MA, Joshi SR, Patil PD, Shejawal KP, Thorat MS, Mulla AS (2020) Formulation and evaluation of Herbal cough remedy from extract of *Calendula officinalis* L. *Indian Drugs* 57(04):52–58
16. Randive DS, Bhutkar MA, Bhinge SD (2020) Formulation and evaluation of Lipstick, Rouge and Eye shadow using colored pigment from the extract of Piper betel and Acacia catechu. *Indian Drugs* 57(02):59–66
17. Randive DS, Bhinge SD, Wadkar GH, Sayyad SF, Bhutkar MA (2016) Comparative standardization of marketed formulations of fermented biomedicine – arjunaristha Indonesian. *J Pharmacoepidemiol* 27:220–225
18. Randive DS, Bhutkar MA, Bhinge SD, Shejwal KP, Patil PD, Mane SA (2019) Hypoglycemic effects of Lagenaria siceraria, Cynodon dactylon and Stevia rebaudiana extracts. *J Herb Pharmacother* 8:51–55
19. Gabetta B, Fuzatti N, Griffini A, Lolla E, Pace R, Ruffilli T, Peterlongo F (2000) Characterization of proanthocyanidins from grape seeds. *Fitoterapia* 71:162–175
20. Kijima I, Phung S, Hur G, Kwok SL, Chen S (2006) Grape seed extract is an aromatase inhibitor and a suppressor of aromatase expression. *Cancer Res* 66: 5960–5967
21. Skerget M, Kotnik P, Hadolin M, Hras AR, Simonic M, Knez Z (2005) Phenols, proanthocyanidins, flavones and flavonols in some plant materials and their antioxidant activities. *Food Chem* 89:191–198
22. Quideau S, Deffieux D, Douat-Casassus C, Pouysegu L (2011) Plant polyphenols: chemical properties, biological activities, and synthesis. *Angew Chem Int Ed* 50:586–621
23. Bagchi D, Bagchi M, Stohs SJ, Das DK, Ray SD, Kuszynski CA, Joshi SS, Pruess HG (2000) Free radicals and grape seed proanthocyanidin extract: importance in human health and disease prevention. *Toxicology* 148:187–197
24. Kim H, Hall P, Smith M, Kirk M, Prasain JK, Barnes S, Grubbs C (2004) Chemoprevention by grape seed extract and genistein in carcinogen-induced mammary cancer in rats is diet dependent. *J Nutr* 134: 3445S–3452S
25. Seeram NP, Adams LS, Hardy ML, Heber D (2004) Total cranberry extract versus its phytochemical constituents: antiproliferative and synergistic effects against human tumor cell lines. *J Agric Food Chem* 52:2512–2517
26. Vayalil PK, Mittal A, Katiyar SK (2004) Proanthocyanidins from grape seeds inhibit expression of matrix metalloproteinases in human prostate carcinoma cells, which is associated with the inhibition of MAPK and NF kappa B. *Carcinogenesis*. 25:987–995
27. Hong H, Yi-Min Q (2006) Grape seed proanthocyanidin extract induced mitochondria-associated apoptosis in human acute myeloid leukaemia 14. 3D10 cells. *Chin Med J* 119:417–421
28. King M, Chatelain K, Farris D, Jensen D, Pickup J, Swapp A, O'Malley S, Kingsley K (2007) Oral squamous cell carcinoma proliferative phenotype is modulated by proanthocyanidins: a potential prevention and treatment alternative for oral cancer. *BMC Complement Altern Med* 7:1–12
29. ERasmussen S, Frederiksen H, Struntze Krogholm K, Oulsen L (2005) Dietary proanthocyanidins: occurrence, dietary intake, bioavailability, and protection against cardiovascular disease. *Mol Nutr Food Res* 49:159–174
30. Kaur M, Singh RP, Gu M, Agarwal R, Agarwal C (2006) Grape seed extract inhibits in vitro and in vivo growth of human colorectal carcinoma cells. *Clin Cancer Res* 12:6194–6202
31. Ying YC, Grayson KJ, Patricia IO, Andrew L (2013) Waterhouse, Bioavailability of intact proanthocyanidins in the rat colon after ingestion of grape seed extract. *Agric Food Chem* 61:121–127
32. Engelbrecht AM, Mattheysse M, Ellis B, Loos B, Thomas M, Smith R, Peters S, Smith C, Myburgh K (2007) Proanthocyanidin from grape seeds inactivates the PI3-kinase/PKB pathway and induces apoptosis in a colon cancer cell line. *Cancer Lett* 258:144–153
33. Keen CL, Holt RR, Ioteiza P, Fraga CG, Schmitz HH (2005) Cocoa antioxidants and cardiovascular health. *Am J Clin Nutr* 81:298S–303S
34. Prior RL, Gu L (2005) Occurrence and biological significance of proanthocyanidins in the American diet. *Phytochemistry* 66:2264–2280
35. Katiyar SK (2007) UV-induced immune suppression and photocarcinogenesis: Chemoprevention by dietary botanical agents. *Cancer Lett* 255(1):1–11
36. Seiler N, Chaabi M, Roussi S, Gosse F, Lobstein A, Raul F (2006) Synergism between apple procyanidins and lysosomotropic drugs: potential in chemoprevention. *Anticancer Res* 26:3381–3385
37. Caili FU, Loo AEK, Chia FPP, Huang D (2007) Oligomeric proanthocyanidins from mangosteen pericarps. *J Agric Food Chem* 55:7689–7694
38. Abdel-Mohsen AM, Abdel-Rahman RM, Fouda MMG, Vojtova L, Uhrova L, Hassan AF, Al-Deyab SS, El-Shamy IE, Jancar J (2014) Preparation, characterization and cytotoxicity of schizophyllan/silver nanoparticle composite. *Carbohydr Polym* 102:238–245
39. Phull AR, Abbas Q, Ali A, Raza H, Jakim S (2016) Antioxidant, cytotoxic and antimicrobial activities of green synthesized silver nanoparticles from crude extract of *Bergenia ciliata*. *Future J Pharm Sci* 2:31–36
40. Raju C, Bharadwaj MS, Prem K, Satyanandam K (2016) Green synthesis of iron nanoparticles using *Albizia lebbek* leaves for synthetic dyes decolorization. *Int J Sci Eng Tech Res* 5:3429–3434
41. Bhinge SD, Hogade MG, Savali AS, Hariprassana RC, Magdum CS (2013) Antibacterial activity of bark extract of ficus glomerataroxb against some gram positive and gram negative bacteria. *Indian Drugs* 50:44–47
42. Bhinge SD, Bhutkar MA, Randive DS, Wadkar GH, Todkar SS, Kakade PM, Kadam PM (2017) Formulation development and evaluation of antimicrobial polyherbal gel. *Ann Pharm Fr* 75:349–358
43. Bhinge SD, Bhutkar MA, Randive DS, Wadkar GH, Kamble SY, Kalel PD, Kadam SS (2019) Formulation and evaluation of polyherbal gel containing extracts of *Azadirachta indica*, *Adhatoda vasica*, *Ocimum tenuiflorum* and *Pongamia pinnata*. *J Res Phar* 23(1):44–54
44. Mosmann T (1983) Rapid colorimetric assay for cellular growth and survival: application to proliferation and cytotoxicity assays. *J Immunol Methods* 65: 55–63
45. Mensor LL, Menezes FS, Leitao GG, Reis AS, Dos Santos TC, Coube CS (2001) Screening of Brazilian plant extracts for antioxidant activity by the use of DPPH free radical method. *Phytother Res* 15:127–130
46. Dahlous KA, Abd-Elkader OH, Fouda MMG, AL Othmana ZA, El-Fahama A, (2019) Eco-friendly method for silver nanoparticles immobilized decorated silica: synthesis & characterization and preliminary antibacterial activity, *J Taiwan Inst Chem E* 95: 324–331.
47. Hussein J, El-Naggar ME, Fouda MMG, Morsy OM, Ajarem JS, Almalki AM, Allam AA, Mekawi EM (2020) The efficiency of blackberry loaded AgNPs, AuNPs and Ag@AuNPs mediated pectin in the treatment of cisplatin-induced cardiotoxicity in experimental rats. *Int J Biol Macromol* 159:1084–1093. <https://doi.org/10.1016/j.jbiomac.2020.05.115>
48. Sulaiman GM, Ali EH, Jabbar II, Saleem AH Synthesis, characterization, antibacterial and cytotoxic effects of silver nanoparticles. *Dig J Nanomater Bios* 9(2):787–796
49. Sulaiman GM, Tawfeeq AT, Naji AS (2018) Biosynthesis, characterization of magnetic iron oxide nanoparticles and evaluations of the cytotoxicity and dna damage of human breast carcinoma cell lines. *Artif Cells Nanomed Biotechnol* 46(6):1215–1229. <https://doi.org/10.1080/21691401.2017.1366335>
50. Taha ZK, Hawar SN, Sulaiman GM (2019) Extracellular biosynthesis of silver nanoparticles from *Penicillium italicum* and its antioxidant, antimicrobial and cytotoxicity activities. *Biotechnol Lett* 41:899–914
51. Khashan KS, Sulaiman GM, Mahdi R (2017) Preparation of iron oxide nanoparticles-decorated carbon nanotube using laser ablation in liquid and their antimicrobial activity. *Artif Cells Nanomed Biotech* 45(8):1699–1709. <https://doi.org/10.1080/21691401.2017.1282498>
52. Foudaa MMG, El-Aassar MR, El Fawal GF, Hafez EE, Masry SHD (2015) K-carrageenan /Poly vinyl pyrrolidone/polyethylene glycol/silver nanoparticles film for biomedical application. *Int J Biol Macromol* 74(3):179–184. <https://doi.org/10.1016/j.jbiomac.2014.11.040>

Publisher's Note

Springer Nature remains neutral with regard to jurisdictional claims in published maps and institutional affiliations.